INTERNATIONAL SOCIETY FOR SOIL MECHANICS AND GEOTECHNICAL ENGINEERING

SIMSG ISSMGE

Penetration characteristics of xanthan gum grout in coarse soil matrix

M. Lee, D.Y. Park & G.C. Cho
Department of Civil and Environmental Engineering, Korea Advanced Institute of Science and Technology, Daejeon, Korea

I. Chang
Department of Civil Systems Engineering department, Ajou University, Suwon, Korea

ABSTRACT: Biopolymer-soil treatment (BPST), as a sustainable ground improvement method, has positively affected strengthening, erosion control, and permeability reduction of ground in both lab and field scale tests. For biopolymer treatment using the permeation grouting method, the mobility of biopolymer fluids in porous media and geotechnical engineering performance after injection must be evaluated. In this study, the behavior of shear-thinning biopolymer hydrogel penetrating within sandy soil was experimentally evaluated. The result indicates that the penetrability of biopolymer fluid is affected by ground properties (i.e., mean particle size, relative density, good content, and permeability) and injection pressure, which are related to pressure loss and in-situ viscosity. The result from this study could be utilized as a basis for the design of biopolymer hydrogel grouting.

Keywords: biopolymer hydrogel, ground improvement, grouting, penetration, porous media.

1 INTRODUCTION

Conventional ground improvement materials such as cement, lime, and waterglass-based chemicals have serious concerns about environmental impact (Soldo et al. 2020). As a result, eco-friendly biological approaches have recently been investigated to overcome the concerns and drawbacks of traditional soil-stabilizing materials (DeJong et al. 2010; Chang et al. 2020). Among these options, the use of biopolymers has advantages over other biological soil treatment methods in terms of speed and quantity/quality control (Chang et al. 2016).

In laboratory studies, biopolymer-based soil treatment (BPST) has demonstrated significant soil strengthening, reduction of hydraulic conductivity, and infiltration mitigation (Bouazza et al. 2009; Latifi et al. 2017; Chang & Cho 2019). In addition, field applications for soil surface reinforcement were attempted to confirm the applicability and feasibility of BPTS in the field (Seo et al. 2021).

However, to use BPTS as a permeability control strategy inside a ground or earthen construction rather than on the surface, assessing the compatibility as an injection method (i.e., grouting) is essential. As a result, this study focused on the rheological property and injection capabilities of biopolymer hydrogel into soil media for grouting and hydraulic barrier purposes. Thus, a series of rheological tests and soil injection tests were performed, and the rheology and penetration behavior of xanthan gum biopolymer hydrogel were discussed.

2 MATERIALS AND METHODS

2.1 Xanthan gum biopolymer

Xanthan gum (XG) is an extracellular polysaccharide generated by the bacteria *Xanthomonas campestris* with a high molecular weight (i.e., $2 \cdot 10^6$ ~$2 \cdot 10^7$ Da) (Rochefort & Middleman 1987). XG is a representative non-gelling biopolymer primarily employed in the food, cosmetics, and petroleum industries (Sworn 2021). XG molecule consists of a repeating linear 1,4-D glucose backbone with charged trisaccharide side chains (i.e., two mannose and one glucuronic acid). Because the negative charge of the pyruvic and glucuronic acid groups (i.e., COO-) on the side chains helps XG molecule connect to water molecules, it expands dramatically. It has a high viscosity when dissolved in, even at low concentrations, with temperature and pH stability (García-Ochoa et al. 2000).

2.2 Used soil: sand

This study used three granular sands (i.e., coarse, medium, and fine) with different effective grain sizes (Figure 1). Non-plastic silt, which has an effective grain size of 28 μm and includes 43% of fine (less than 75 μm), was mixed with medium sand to prepare specimens with non-plastic silt content of 5%, 10%, 15%, and 20% (labeled as MS(5), MS(10), MS(15), and MS(20), respectively). The representative index parameters of the soil used in this study are summarized in Table 1.

2.3 Preparation of XG hydrogel

Dried XG powder was dissolved and hydrated in pure

distilled water to make XG hydrogel using a laboratory hand mixer until a uniform hydrogel was achieved. For the rheometry and injection test, the hydrogel recipe was set to the water mass to biopolymer mass ratio (WB) = 16, 20, 27, 40, 53, and 80.

2.4 Rheology measurement of Xanthan gum hydrogel

The yield stress of XG hydrogel is basic properties related to flow characteristics in porous media, such as injectability. Following previous studies, a rotational rheometer (Anton-Paar RheolabQC) with a vane geometry was used to measure the rheology of the XG grout. The vane cup system has a cup with an inner diameter of 29 mm and a four-blade vane spindle with a width of 22 mm and a height of 40 mm. The yield stress was measured using torque-time response under constant shear rate conditions (0.05 s^{-1}). The water mass to biopolymer mass ratio (WB) is 16, 20, 27, 40, 53, and 80.
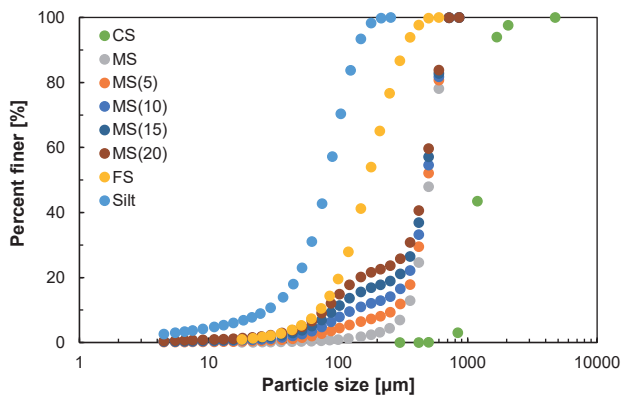

Fig. 1. Particle size distribution of used soils.

Table 1. Soil index parameters

Sand	G_s	D_{10} (μm)	C_u	C_c	USCS
CS	2.64	900	1.50	0.95	SP
MS	2.65	331	1.63	1.08	SP
MS(5)	N/A	265	1.99	1.27	SP
MS(10)	N/A	131	3.96	2.38	SP-SM
MS(15)	N/A	93	5.49	3.04	SP-SM
MS(20)	N/A	79	6.38	3.12	SP-SM
FS	2.66	72	2.72	1.10	SP-SM
Silt	2.67	28	3.32	1.43	SM

Note: USCS, Unified Soil Classification System (ASTM 2011); SP, poorly graded sand, SP-SM, poorly graded sand with silt; SM, Silty sand; N/A, not available (not tested)

2.5 Injection test

The parameters that influence the penetrability of XG grout in granular soil were evaluated using constant pressure injection tests. These injection tests were used to investigate the penetration distance and stop mechanism of the XG grout through various sand columns.

The overall schematic diagram of the injection test setup is shown in Figure 2. The system is composed of a cylindrical grout chamber, pressure panel, air compressor, and permeation cell. Permeation cell is consists of a cylinder with a diameter of 7 cm and a height of 28 cm, a base plate, and a top cap. To avoid soil media clogging the injection hole, a wire meshes finer than soil grains was placed on the bottom plate. The upper cap, which restricts and prevents the uplift of soil specimens, is positioned at the top of the permeation column (above the soil), and it includes a hole through which water and grout flow out.

Clean sands (i.e., fine, medium, and coarse sand) and sand-silt mixture (i.e., medium sand with 5~20% of silt) were prepared with desired density in permeation cell. The calculated porosity and density of soil media are assumed to be the average value along the length of the sand column. Prepared sand columns were saturated with slow flushing of de-aired water from the bottom to top.

XG hydrogel was also made similar to the rheological test, placed immediately in the grout chamber after mixing. At constant pressure conditions (i.e., 37 to 300kPa), various WB grouts were injected into the sand column. The effluents during injection were collected in a beaker, and the weight of the grout chamber was measured simultaneously to determine grout intake. The grout intake was monitored for about 10 minutes after injection.

3 EXPERIMENTAL RESULTS AND ANALYSIS

3.1 Rheology of xanthan gum hydrogel

After preparing XG hydrogel, a series of constant shear rate tests were performed with various WB. The yield stress can be estimated using the below equation suggested by Dzuy and Boger (1985) (Dzuy & Boger 1985).

$$\tau_y = \frac{2}{\pi D^2} \left(\frac{H}{D} + \frac{1}{3} \right)^{-1} T_{max} \qquad (1)$$

where τ_y is yield stress, D is the width of the vane, H is the height of vane, T_{max} is the maximum torque.
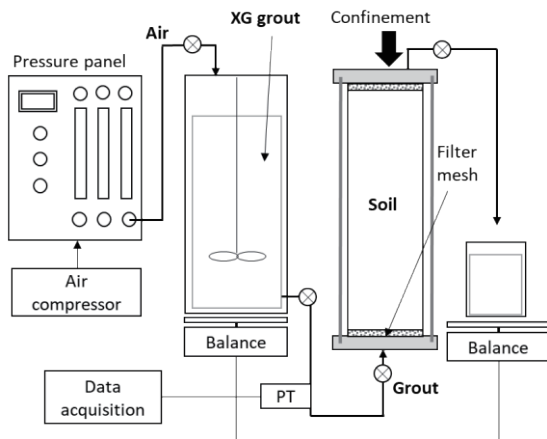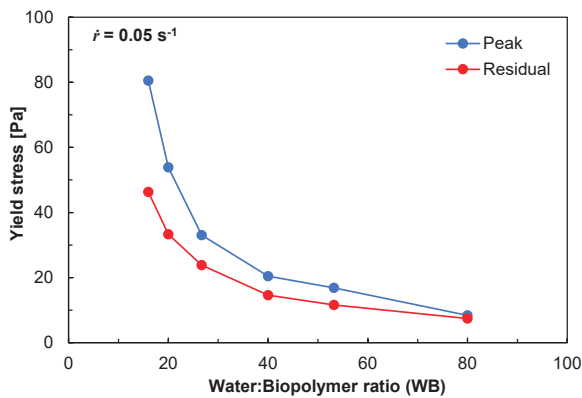
Fig. 2. Schematic setup of injection test

Fig. 3. Yield stress by water:biopolymer (WB) ratio

The static and dynamic yield stress values gradually decreased from 80 Pa to 8 Pa, and 46 Pa to 7 Pa for the WB range increased from 18 to 80 (Figure 3)

3.2 Injection behavior

The influence of various parameters (i.e., WB, soil grain size, silt content, and injection pressure) on penetrability was evaluated by injecting XG hydrogel into sand columns. The variation in grout intake with injection time was measured to analyze the response and final penetration distance of injected flow. Figure 4a presents the maximum penetration distance according to the WB ratio. The penetration distance increases as a power function as the WB ratio increases. The increase of penetration distance with WB ratio is observed in similar range regardless of mean size particle in soil media. For example, the penetration distance increased by about 4.1 times, 4.5 time, and 4.3 time in FS, MS, and CS, respectively, when WB was increased from 20 to 80.

On the other hand, the penetration distance of XG hydrogel increases linearly with the injection pressure. However, as more silt was included in the same medium sand, it was observed that the penetrability decreased in the form of power.
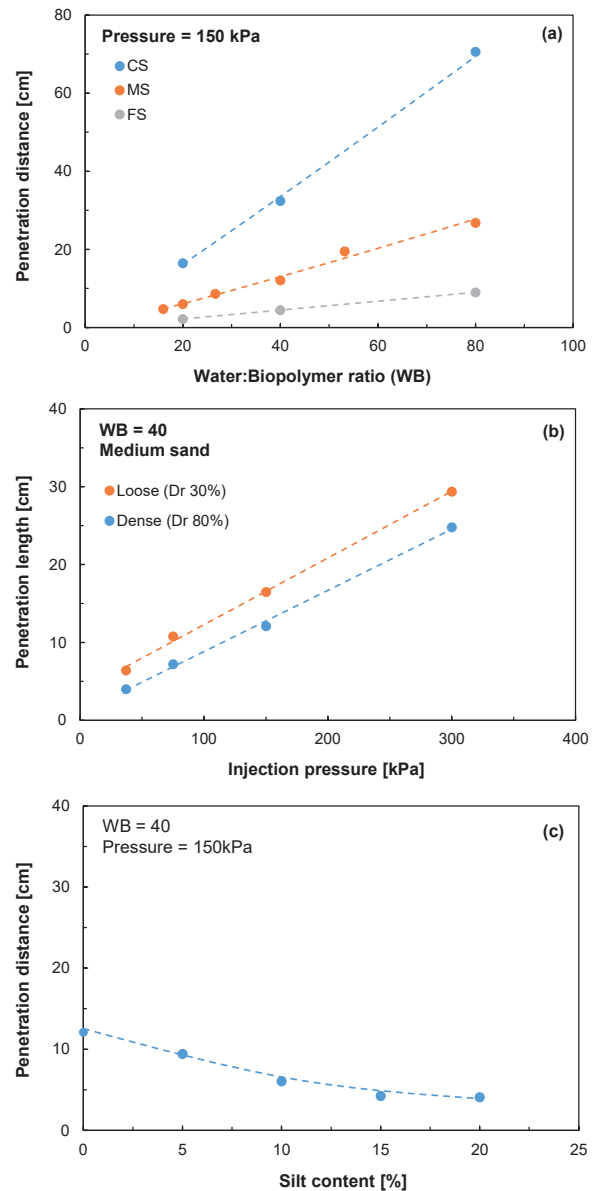
Fig. 4. Injection test result. (a) penetration distance by WB and soil type. (b) penetration distance by injection pressure. (c) penetration distance by silt content

4   DISCUSSIONS

It is well known that XG hydrogel exhibits shear thinning behavior that the viscosity markedly reduces with a high shear rate. This shear-thinning behavior is originated from tenuous gel-like (i.e., weak) networks built by associated XG molecules via hydrogen bonding. When a high shear force is applied to these networks, the viscosity of XG hydrogel decreases rapidly. In addition, the stress required to initiate the flow (i.e., viscosity reduction) is static yield stress. As the WB decreases, the yield stress increases, adversely affecting XG hydrogel penetration under the same pressure. Figure 5 presents the penetration distance with a yield stress, indicating

that penetrability decreases in a power-law relationship. The estimated penetration length using the theoretical penetration model of Bingham grout, which has yield stress, proposed by Axelsson et al. 2009 (Axelsson et al. 2009), was compared with experimental data. The penetration length from the injection test result is well-fitted with the theoretical model.

$$I_{max} = \frac{\Delta P}{\tau_y} \frac{4}{\pi(1-n)S} \tag{2}$$

where I_{max} is penetration distance, ΔP is pressure, τ_y is yield stress of grout, n is soil porosity, and S is the specific surface of the soil.

The infiltration and clogging behavior is a major stop mechanism for conventional particulate grout suspensions (i.e., cement and bentonite). However, in the case of XG, the molecular size in polymer hydrogel is about 4μm, which is smaller than other grout particle sizes (Unsal et al. 1977). Thus it can be expected that infiltration blocking hardly occurs during injection of XG hydrogel. When injecting the XG-based grout, a drag force at the pore surface due to high yield stress and viscosity hinders the penetration by dissipating the energy and reducing the pressure gradient. As the shear rate applied on XG grout decreased, its high viscosity and yield stress recovered. As a result, XG grout no longer penetrates and becomes a stable state in the pore, maintaining lower soil permeability.
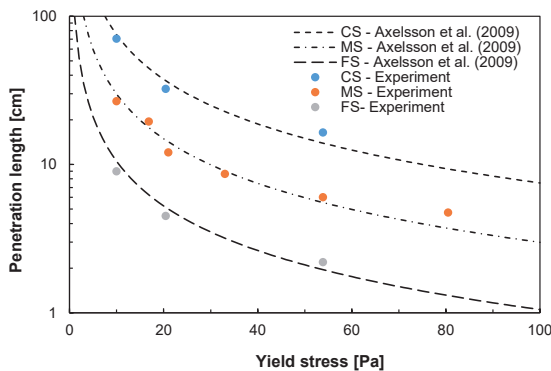

Fig. 5. The penetrability of XG grout by yield stress and comparison between the theoretical and experimental result

5 CONCLUSIONS

This study focuses on the rheological property and penetration capabilities of highly concentrated XG grout for grouting purposes. Results showed that rheology and soil conditions could hinder the efficiency of injection. owever, the high yield stress of XG enables the pore filling XG hydrogel to maintain stability as a permeability control strategy.

REFERENCES

Axelsson, M., Gustafson, G. and Fransson, Å. 2009. Stop mechanism for cementitious grouts at different water-to-cement ratios. *Tunnelling and Underground Space Technology*. 24(4), 390-397.

Bouazza, A., Gates, W. and Ranjith, P. 2009. Hydraulic conductivity of biopolymer-treated silty sand. *Geotechnique*. 59(1), 71-72.

Chang, I. and Cho, G.-C. 2019. Shear strength behavior and parameters of microbial gellan gum-treated soils: from sand to clay. *Acta Geotechnica*. 14(2), 361-375.

Chang, I., Im, J. and Cho, G. C. 2016. Introduction of microbial biopolymers in soil treatment for future environmentally-friendly and sustainable geotechnical engineering. *Sustainability*. 8(3), 251.

Chang, I., Lee, M., Tran, A. T. P., Lee, S., Kwon, Y.-M., Im, J. and Cho, G.-C. 2020. Review on biopolymer-based soil treatment (BPST) technology in geotechnical engineering practices. *Transportation Geotechnics*. 24 100385.

DeJong, J. T., Soga, K., Banwart, S. A., Whalley, W. R., Ginn, T. R., Nelson, D. C., Mortensen, B. M., Martinez, B. C. and Barkouki, T. 2010. Soil engineering in vivo: harnessing natural biogeochemical systems for sustainable, multi-functional engineering solutions. *Journal of the Royal society Interface*.

Dzuy, N. Q. and Boger, D. V. 1985. Direct yield stress measurement with the vane method. *Journal of Rheology*. 29(3), 335-347.

García-Ochoa, F., Santos, V., Casas, J. and Gomez, E. 2000. Xanthan gum: production, recovery, and properties. *Biotechnology Advances*. 18(7), 549-579.

Latifi, N., Horpibulsuk, S., Meehan, C. L., Majid, M. Z. A., Tahir, M. M. and Mohamad, E. T. 2017. Improvement of problematic soils with biopolymer - An environmentally friendly soil stabilizer. *Journal of Materials in Civil Engineering*. 29(2), 04016204.

Rochefort, W. E. and Middleman, S. 1987. Rheology of Xanthan Gum: Salt, Temperature, and Strain Effects in Oscillatory and Steady Shear Experiments. *Journal of Rheology*. 31(4), 337-369.

Seo, S., Lee, M., Im, J., Kwon, Y.-M., Chung, M.-K., Cho, G.-C. and Chang, I. 2021. Site application of biopolymer-based soil treatment (BPST) for slope surface protection: in-situ wet-spraying method and strengthening effect verification. *Construction and Building Materials*. 307 124983.

Soldo, A., Miletić, M. and Auad, M. L. 2020. Biopolymers as a sustainable solution for the enhancement of soil mechanical properties. *Scientific Reports*. 10(1), 267.

Sworn, G. (2021), *Chapter 27 - Xanthan gum in Handbook of Hydrocolloids*, Woodhead Publishing

Unsal, E., Duda, J. L., Klaus, E. E. and Liu, H. T. (1977). "Solution properties of mobility control Polymers", *SPE Eastern Regional Meeting*.